Serbian Tribology Society

SERBIATRIB '13

13th International Conference on Tribology

Faculty of Engineering in Kragujevac

Kragujevac, Serbia, 15 – 17 May 2013

PRELIMINARY STUDY ON THE SEIZURE TREND OF A MOM-THP WITH SELF-DIRECTED BALLS

Lucian Capitanu[1], Liliana – Laura Badita[2], Virgil Florescu[2], Dumitru Catalin Bursuc[3]

[1]Institute of Solid Mechanics of the Romanian Academy, 15 Constantin Mille, 010141, Bucarest, Romania luciancapitanu@yahoo.com

[2*]National Institute for Research and Development in Mechatronics and Measurement Technique, 6-8 Sos Pantelimon, district 2, Bucharest, Romania badita_l@yahoo.com

[3]Mechanical Departament, Institute of Civil Engineering, 59 Plevnei Way, 050141, Bucharest, Romania, florescuvirgil@yahoo.com

[4]"Carol I" National Defance Academy, Bucharest, Romania, catalin258@yahoo.com

Abstract: *This work continues the approach of one of our topics relating to a MOM THP with self-directed movement balls. Experiments revealed a certain seizure in some strain conditions. Laboratory trials for balls/plane Hertzian contacts have been restarted in order to determine seizure behaviour depending on the roughness of the flat area. The trials have been carried out in BSF (body simulated fluid) lubrication conditions, much closer to the real operating conditions up against the initial tests with distilled water. Seizure burdens to different loadings and contact surfaces roughness influence over the seizure burden have been determined. Even though the minimum value of the wear must be the same with the minimum value of the surfaces roughness, given the experimental conditions, it came out from the trials results on wear that the lowest level of wear is acquired at a certain value of roughness, not at the lowest level of roughness.*

Keywords: *MOM –THP with balls, self-directed movement, seizure, optimal conditions, wear scar, friction coefficient.*

1. INTRODUCTION

Nowadays, the design solutions for Total Hip Prostheses are diverse encompassing for improving the materials used for prostheses elements and reshaping geometrically and/or tribologically the load transfer path. In such context Total Hip Prostheses with rolling balls have been found as a possible viable alternative design to current industrial products, based on low friction of rolling contact, against sliding one (now used in most industrial designs).

Different designs of Total Hip Prostheses with Different designs of Total Hip Prostheses with rolling bodies have been developed in order to improve the tribological performances of the artificial joint. We could mention here the design with ball train, proposed by Katsutoshi and Kiyoshi [1], the French "Supertête" prosthesis [2], or the design with conical rolling elements proposed by Imperial College of Science, Technology and Medicine of London [3].

The French design, obtained by "Fondation de l'Avenir" in collaboration with "Ministère de la Défense, Mission Innovation", propose the insertion of a frictional contact inside a bearing. The design suggested by Imperial College of Science, Technology and Medicine of London consists in a major modification of a elements between the femoral part stem neck and the modular hip prosthesis by introducing a rolling bearing with conical femoral artificial head.

The bearing rotation axis corresponds with the axis of femoral stem neck, the rolling elements being guided by both the external surface of stem neck and the internal surface of the ball replacing the femoral head. But changing the contact mechanism from sliding to rolling in a hip prosthesis is not an easy task due to difficulties encountered in establishing the load transfer path, a critical characteristic of tribological behavior of joint with large influence in functionality and durability of prosthesis active elements.

Basically, the sliding contact between large surfaces of femoral head and acetabular cup was replaced by a multitude of rolling contacts with a different pattern of stress distribution influenced by rolling elements position at some instant during relative movement between femoral and acetabular parts.

In the present paper, the authors focus on the original design proposed by them in [4], *i.e.* a MOM Total Hip Prosthesis with self directed rolling balls (see Fig. 1).

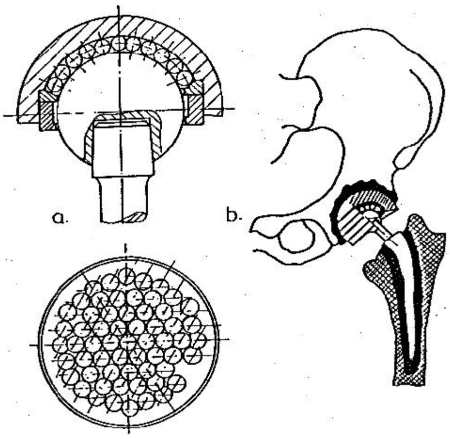

Figure 1. Total Hip Prosthesis with self directed rolling bodies.

A characteristic of this design solution is the fact that the artificial joint will work similar to a spherical bearing, having what is called a “compensation space”, *i.e.* enough free space between the femoral and acetabular parts of the prosthesis to allow the movement of the balls [5].

Previous research studies performed by the authors focused on the determination of the initial position of rolling balls due to geometrical restraints of the assembly and on the estimation of the overall friction coefficients in dry and lubricated motion [5].

The geometrical studies (see [6] and [7]) have shown that generally the balls are located non-symmetrically and that the configuration for a given space and a given number of balls is not unique. Tribological studies performed by he authors (see [4], [6] and [7]) have shown very low values of overall friction coefficients (0.12 to 0.2 for dry joint and 0.006 to 0.009 in the presence of lubricants), leading to an enhanced functionality of the prosthesis itself. The present study will use the results of the previous studies in order to determine the load distribution through the balls bed and the compressions generated between the joint elements (femoral head, rolling balls, acetabular cup).

As we previously stated, a general study of the proposed design will target the following mechanical aspects:

– characterization of load transfer mechanism through the joint elements (statics of enveloping loads and/or dynamics studies of natural, physiological movements);

– evaluation of tribological behavior of all joint elements (including contact mechanics of all active interfaces – femoral head-ball, ball-ball, ball-acetabular cup);

– estimation of functional threats and damaging mechanisms for the proposed design (*i.e.* clear definition of criteria for joint locking, fatigue of prosthetic parts, wear of active elements of the joint) and determination of influencing factors for all these unwanted phenomena.

Lessons learned from previous attempts (structural overall analysis performed in [8]) lead to decoupling the statics and dynamics of the joint (FE analyses) from the tribological behavior (separate analytical evaluation) in order to save computational effort and assuming simplifications. The characteristics of the prosthesis under evaluation are as follows:

- type: Total Hip Prosthesis (THP) with self directed rolling balls;
- geometrical features: outer radius of femoral head - 14 mm; radius of each rolling ball 1.25 mm; internal radius of acetabular cup - 16.5 mm; spherical cap for balls bed (subtended angle) - 160°;

Material used for components:

- femoral head - Stellite 21;
- acetabular cup - Ti6Al4V;
- rolling balls - CoCrMo alloy.

The methodology used for computing the number of balls needed for assembling the joint and their positions inside the artificial joint is that used in [4]. The resulted configuration of artificial joint was used in order to build the numerical model for load transfer path through the balls bed.

The 3D numerical model is a large one – 58,784 elements and 73,100 nodes, with numerous surfaces in contact, requiring high computational resources and significant time for simulation. Instead of using a big model with multiple non-linearities, a simplified model was built based on the following assumed hypotheses

1. Femoral head and balls have been considered rigid (their stiffness is much higher than acetabular cup stiffness).
2. The compressive force and flexion drive moment have been maintained constant.
3. Linear elastic behavior of acetabular cup was assumed.
4. The compressive forces acting at the ball-to-ball contact surfaces are smaller than the compressive forces between balls and femoral head, respectively between balls and acetabular cup. This

assumption allows us to use, instead of spherical balls, unidimensional nonlinear elements (compression only) connecting the spots of contacts between the balls and cup, respectively between the ball and femoral head with the center of each ball.

The train of balls was not actually modeled as it is; instead of 3D representation of the balls (Fig. 5), unidimensional contact elements have been considered between the center of each ball and the active surfaces of femoral and acetabular prosthetic elements.

2. SIMULATION METHODOLOGY AND RESULTS

The 3D FE model was loaded by a compressive 1 kN force and a flexion of the joint was considered for ~37.6° (i.e. a relative maximum displacement of circumferential points located on femoral head and acetabular cup equal with 4 times the diameter of one rolling ball).

After the loads on each ball have been determined (being categorized based on balls regions rather than each ball itself) a local analysis was performed for establishing the extreme Hertzian contact parameters based on the following methodology [9]:

- maximum pressure, given by

$$p_0 = \sqrt[3]{\frac{6PE^{*2}}{\pi^3 R^2}}, \tag{1}$$

- radius of contact spot, given by

$$p_0 = \sqrt[3]{\frac{6PE^{*2}}{\pi^3 R^2}}, \tag{2}$$

- mutual approach between bodies in contact, given by

$$\delta = \sqrt[3]{\frac{9P^2}{16RE^{*2}}}, \tag{3}$$

where P is the applied compressing load, and R the relative curvature given by:

$$\frac{1}{R} = \frac{1}{R_1} + \frac{1}{R_2} \tag{4}$$

After performing the geometrical assessment, based on the methodology presented in [4], it results that the maximum number of balls needed for the spherical joint is 199, distributed on 12 consecutive rows [9] as follows:

$n_0 = 37$; $n_1 = 19$; $n_2 = 19$; $n_3 = 19$; $n_4 = 19$; $n_5 = 19$; $n_6 = 19$; $n_7 = 19$; $n_8 = 14$; $n_9 = 9$; $n_{10} = 5$; $n_{11} = 1$.

Images of the rolling balls positions for $\varphi = 0$ and $\beta = 0° \pm 15°$ (where φ and β are the azimuth and zenith angular coordinates in the spherical coordinate system associated with the femoral head). One could notice from the results of the mathematical analysis that the arrangement of the balls in the rolling space is asymmetrical and will not be uniquely determined.

After applying 1 kN compressive load onto the artificial joint having the balls train configured as resulted from the geometrical analysis [8], the loadings on each rolling ball during the 37.6° flexion were determined by FE analysis of a dynamic nonlinear model of the entire joint. Several three instances have been selected for presenting the results in both vertical a nd normal views to the flexion plane in Figs. 2.

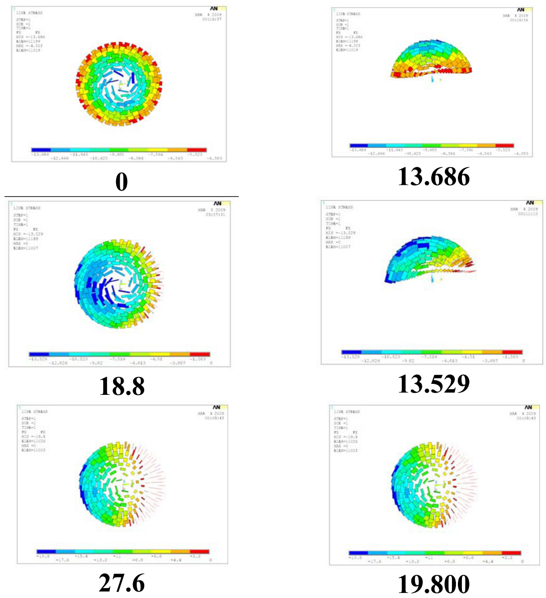

Figure 2. The compressive loadings transferred from femoral to acetabular parts of the prosthesis for different instances of flexion (between 0° and 37.6°); flexion listed in left, maximum load listed in right part of the pictures).

Its correspond to 1 - diameter, 2 - diameter, 3 - diameter and 4 - diameter relative displacements between the acetabular and femoral parts of the prosthesis.

By analyzing the plots, the following conclusions could be drawn:

a. Even for the initial condition, due to asymmetrical arrangement of the balls resulted from the geometrical analysis, there is some asymmetry of transferring the load path from the femoral head to the acetabular part [8].

b. During the flexion (especially for large angles) a part of the balls will not be loaded anymore, leading to an increase of the maximum force transmitted by intermediate of a rolling ball (from ~1.35% of the total joint compression force - as for flexion angles lower than 18.8°, to ~1.98% of the total joint compression force - as for a flexion of 37.6°) - Fig.2.

c. By analyzing the loading of each ball row, it has been determined (for the initial position, 0°

flexion) that the most loaded rows are those located close to 40°…60° from the equatorial plane (the rows located lower have small loads on each balls, and for the rows located higher each ball carries a bigger load but the number of balls is low). The distribution of rolling balls loading versus the zenith positioning angle of the rolling ball is presented in Fig. 3.

Analyzing the graph, the following conclusions could be drawn:

1. As reported before, there is a slight asymmetry of the distribution even for the initial position. This asymmetry evolves with flexion leading to unloading of some balls located peripherally outside the hemispherical area characterized by compressive loading pole.

2. The peripheral balls located closer to the compressive loading pole are generally highly loaded, but the highest loaded balls remain those positioned in intermediate rows (between 40° and 60° from the equatorial plane).

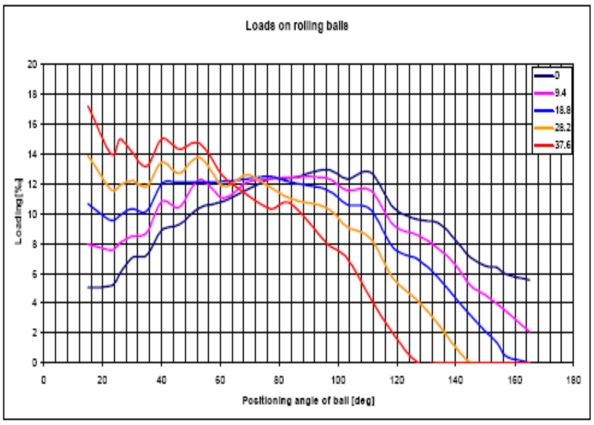

Figure 3. The rolling balls loadings versus zenith positioning angle of ball.

For the extreme maximum loadings of the balls during the analyzed flexion, a preliminary evaluation of tribological parameters of contact between femoral head and rolling balls and between rolling balls and acetabular cup has been performed by using formulae (1) - (3).

3. LABORATORY TRIALS

Experiments revealed a certain seizure in some strain conditions. Laboratory trials for balls/plane Hertzian contacts have been restarted in order to determine seizure behaviour depending on the roughness of the flat area. The trials have been carried out in BSF (body simulated fluid) lubrication conditions, much closer to the real operating conditions up against the initial tests with distilled water.

Seizure burdens to different loadings and contact surfaces roughness influence over the seizure burden have been determined.

Even though the minimum value of the wear must be the same with the minimum value of the surfaces roughness, given the experimental conditions, it came out from the trials results on wear that the lowest level of wear is acquired at a certain value of roughness, not at the lowest level of roughness.

For the tests we used the test rig presented in Fig. 4. In this test rig, the friction pair is formed from a bush with spherical profile and a flat disk shaped with a diameter of 18 mm and a thickness of 5 mm (see Fig. 5). The sphere's radius is r = 11.5 mm.

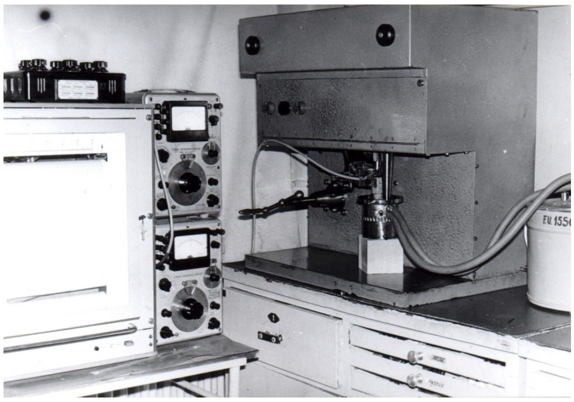

Figure 4. Experimental test rig

Figure 5. Used friction couple

In the static contact, compression stresses in contact spot, p_{max} si p_{med} (maximum pressure and mean pressure) are:

$$p^3_{max} = 1.5\ PE^2 / \pi\, r^2\, (1-\mu^2)^2 \qquad (5)$$

$$p_{med} = \frac{P}{\pi a^2} \qquad (6)$$

and the radius of the contact surface, a, is:

$$a^3 = 1.5\left(1-\mu^2\right)P\frac{r}{E} \qquad (7)$$

where P is the load, a – radius of the contact surface, and r – radius of the sphere.

In the friction couple components (see Fig. 9) are made of steel, the quantities of equations (5), (6) and (7) become:

$$p_{\max} \approx 5800 \sqrt[3]{P} \tag{8}$$

$$p_{\text{med}} \approx 1700 \sqrt[3]{P} \tag{9}$$

$$a \approx 0.09 \sqrt[3]{P} \tag{10}$$

Attention was paid to processing of working surfaces of couples. Surface state defined by topography, microstructure of surface layer and oxidation state has a major influence on the wear process.

Due to the complexity of processing by abrasion of the surface, the most reliable way to ensure a reproductible surface is stringently observance of all processing phases, which are turning of the form, finishing turning, thermal treatment, and correction of profile by polishing and superpolishing of working surface.

All the operations until smooth processing of the profile are made by current technology, noting that the intensity of the process is kept low to protect the structure of the surface layer of material.

Super-finishing operation using metallographic ground slides technique includes:

- wet polishing with sandpaper, grain size 32 µm and 17 µm;
- polishing with diamont slury, grain size 6 µm and 1 µm;
- wet polishing with slury of 2000 Å.

Finally, the surfaces are washed with distiled water, alcohol and then are dried.

The maintenance of processed couples is made in closed vessels, on silica gel. Surfaces roughness was measured with a roughness tester with parametric transducer and recording. The instrument allow recording of surface profile, and also determination of R_a and *r.m.s.*, defined as:

$$R_a = \frac{1}{l}\int_0^l |y|dx \tag{11}$$

$$r.m.s = \sqrt{\frac{1}{l}\int_0^l y^2 dx} \tag{12}$$

In Fig. 6 (A1-A8) profiles (cross-cut) of the surfaces used and of microphotographs obtained in normal lighting are presented.

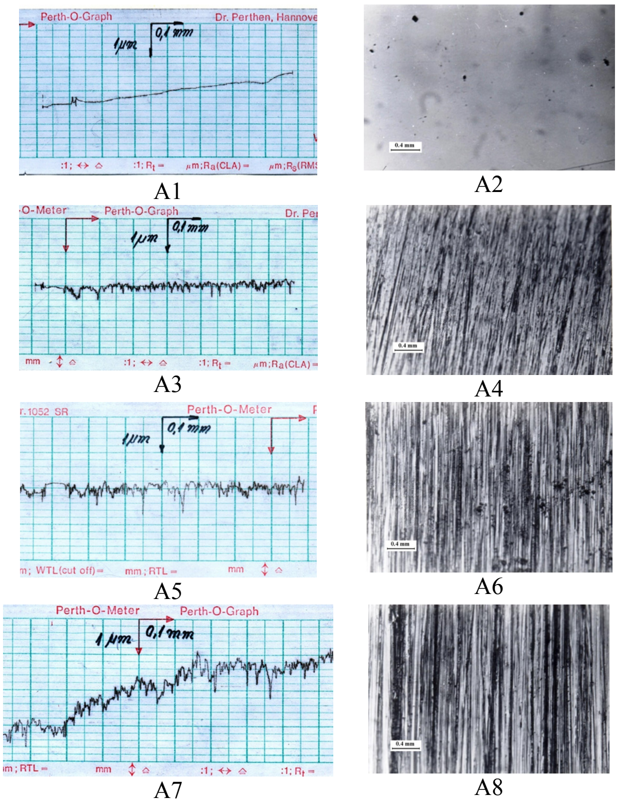

Figure 6. Profile and microfotograph of the surface with roughness R_a = 0.015 µm (A1-A2), R_a = 0.045 µm (A3-A4), R_a = 0.075 µm (A5-A6) si R_a = 0.19 µm (A7-A8).

4. RESULTS AND DISSCUSION

4.1. Evolution of the surface state in the wear process

Experimental determinations were made on these test conditions:

- Load: variabile between P = 20 ÷ 300 N for determining of seizure limit. A load of 50 N was used for wear tests.
- Sliding speed: Main speed for determining the wear rate was u = 174 cm/s. To determine the influence of speed on the wear, the device allows achieving speeds:

u = 60 cm/s; u = 18 cm/s si u = 3,2 cm/s.

- Lubricant: BSF (Body Simulated Fluid) with the density 1183 kg/m^3 and vascosity 0.84 Pa s (HyClone, SH30212.03).

Using the parameters above mentioned, the cpuple operates in elastohydrodynamic regime.

For the minimum thickness of the lubricant film, Archard [8] proposed the relationship:

$$\frac{h_0}{r} \approx 0.84\left(\frac{\alpha u \mu_0}{r}\right)^{0.741}\left(\frac{Er^2}{P}\right)^{0.074} \tag{13}$$

where: h_0-minimum thickness of lubricant film; r-radius of the sphere; α-pressure coefficient of vascosity; u-sum velocity; μ_0-dynamic viscosity at atmospferic pressure; E-reduced elasticity modulus; P-load.

Relation (13) reproduces satisfacatory the dependence of h_0 by the main quantities u, μ_0, r and P. The exact determination of the minimum lubricant film thickness depends on the knowledge of pressure coefficient α for lubricant used and the accuracy of the numerical coefficient of relationship (13). In working conditions, using an estimated value α, resulted a minimum lubricant film thickness $h \approx 0.06$ μm.

Spatial form of lubricant film in the loaded area results from Fig. 7 and 8, which represents two sections of lubricant film, longitudinal and cross sections (in relation to the movement) by the symetry axes.

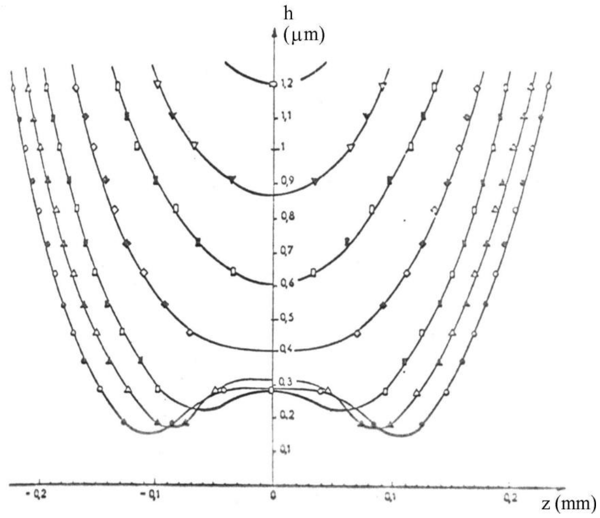

Figure 7. Variation of lubricant thickness in the $x = 0$ plane, function of load, at speed u = 8 cm/s.
▪ 0.7 N; ▼ 1.1 N; □ 1.5 N; ◊ 3 N; ▪ 4.6 N; ▲ 7.8 N; ○ 10.8 N.

Curves were obtained experimentally, under close conditions to those used by Dowson [9]. Are noticed significantly higher values for minimum thickness h_0, even at speed u = 23 cm/s.

To watch in good conditions the wear of fixed surface, function of couple roughness, the following solution was used: roughness of the couple was focused on one of surfaces, in particular on themobile one. Fixed surface had always the minimum roughness achievable, meaning about $R_a \approx 0.015$ μm.

As it is known, the composed roughness of the couple, expressed as standard deviations, σ, is:

$$\sigma^2 = \sigma_1{}^2 + \sigma_2{}^2 \tag{14}$$

where σ_1, σ_2 represent the standard deviations of the two surfaces.

If one of the surfaces has small roughness, i.e. $\sigma_1 << \sigma_2$, then $\sigma \approx \sigma_1$. So it is possible to study the influence of roughness on the wear, just by changing the roughness of the of a single surface.

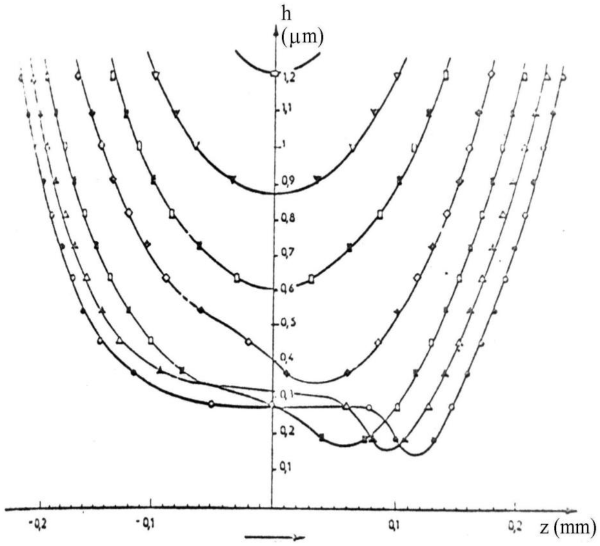

Figure 8. Variation of lubricant thickness in the $z = 0$ plane, , function of load, at speed u = 8 cm/s.
▪ 0.7 N; ▼ 1.1 N; □ 1.5 N; ◊ 3 N; ▪ 4.6 N; ▲ 7.8 N; ○ 10.8 N.

Under these conditions and at a load P = 50 N, speed u = 1.74 m/s and volume temperature of the lubricant $\theta = 50\ ^0$C, it vas determined the evolution of the surface wear function of the time, for the following roughness of the mobile surface: R_a = 0.015 μm; R_a = 0.045 μm; R_a = 0.075 μm si R_a = 0.19 μm.

In Fig. 9 are selectively presented, some wear marks obtained under some condititions mentioned above (at time t = 5 min.), to estimate the results reproductibility.

The worn volume for the three experimental determinations is:

E 1057; $V = 8.50 \times 10^{-5}$ mm^3;
E 1058; $V = 6.11 \times 10^{-5}$ mm^3;
E 1059; $V = 4.00 \times 10^{-5}$ mm^3;

$$\overline{V} = 6.2 \times 10^{-5}\ \text{mm}^3.$$

Determinaations on several samples resulted in an average $\overline{V} = 6.2 \times 10^{-5}$ mm^3. for wear determinations, a deviations of 25% is completely satisfacatory.

Fig.10, shows the wear evolution function of time, for roughness of the bush R_a = 0.045 μm. Time of 3 sec., 1 min., and 5 min., was selected, each made with another couple. For roughness R_a = 0.015 μm, the wear evolution depending on the time was determined with same bush, the total running in time on the scar being divided into intervals of 1, 5 or 10 min. We chose this solution to monitor also the alteration of the bushis surface status. Fig. 10 shows that, except the first 5 min., wear remains at same level.

In Fig. 11 are presented the transversal profile and the image of wear imprint for sample with R_a = 0.045 μm, t = 5 min. (sample 703); R_a = 0.045 μm, t = 5 min., but with bush from the previous determination (total running in time t = 10 min., (sample 704); R_a = 0.045 µm, t = 5 min., with the bush from the previous determination (total running time t = 20 min. (sample 705).

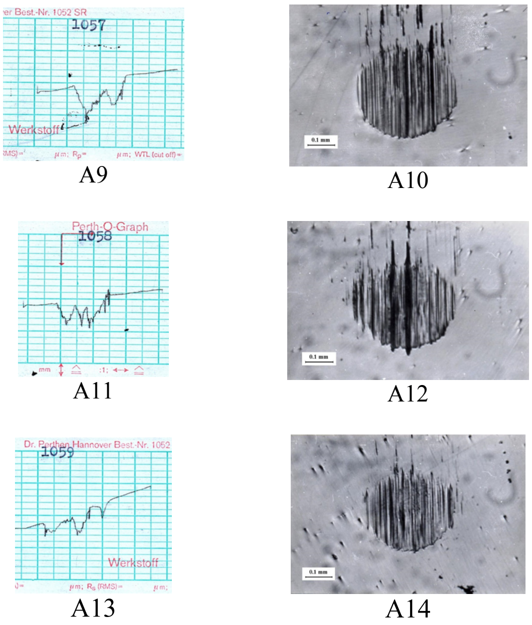

Figure 9. Central transversal profile and image of wear scar (magnification x 68). R_a = 0.015 µm, t = 5 min.

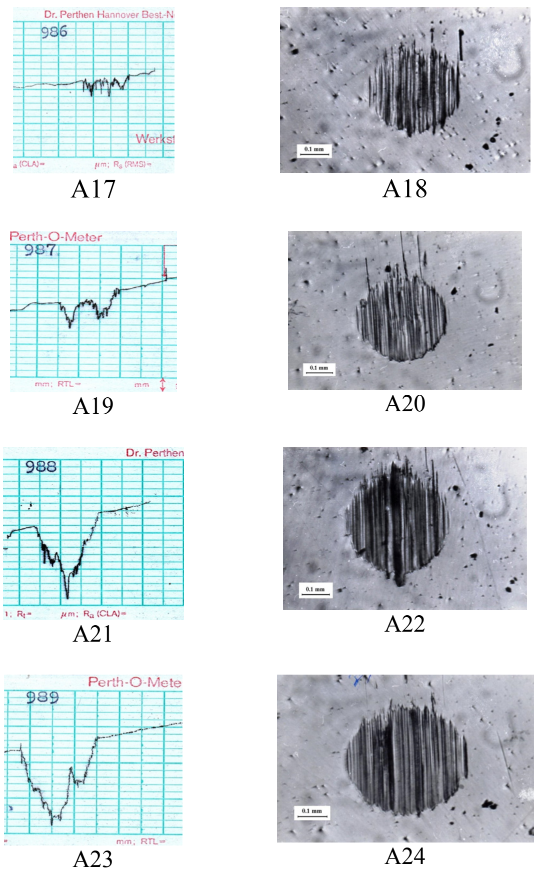

Figure 10. Central transversal profile and image of wear scar (magnification x 68). R_a = 0.045 µm, t = 5 min

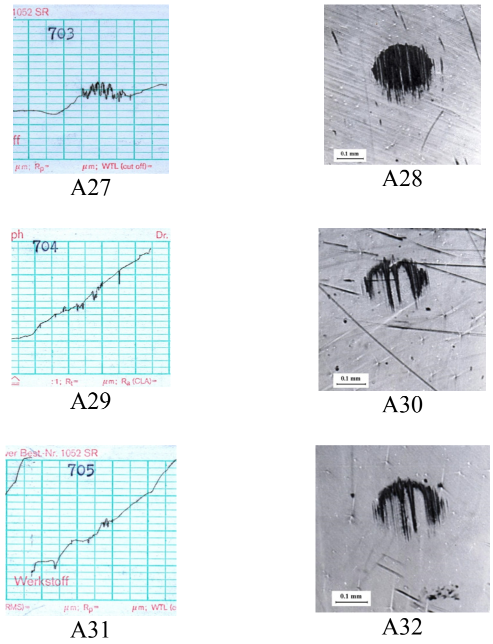

Figure 11. Transversal profile and image of wear imprint for samples with R_a = 0.045 µm, t = 5 min. (sample 703); R_a = 0.045 µm, t = 5 min., but the bush from the previous determination (total running in time t = 10 min. (sample 704); R_a = 0.045 µm, t = 5 min., but the bush from the previous determination ((total running time t = 20 min. (sample 705).

Wear evolution depending on the time for different roughness is shown in Fig. 12. By increasing the running time from 5 min., to 30 min., the wear does not increase only about 10%.

Is noted the rapid reduction of wear rate function of time, except the surface with roughness R_a = 0.045 µm. In the first 3 seconds it is produced between 25% and 50% of wear at 30 min. This wear evolution explained by complying surfaces, which results in changing the lubrication regime.

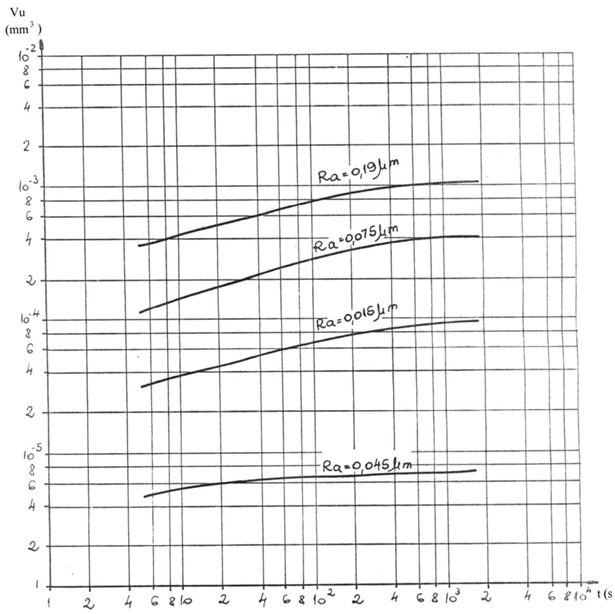

Figure 12. Wear evolution function of time, for different roughness.

Note that the amount of wear on the plateau is caused by the initial wear (during the first few seconds of operaton). This observation allows the use of wear value at t = 5 min., as representative quantity for the existing operating conditions. At this time of operation, scattering of values is lover.

In the case of surfaces with R_a = 0.045 µm, the wear is so low that during the entire period of time used, lubrication conditions remain aproximately unchanged.

Evolution of the wear function of time, for roughness R_a = 0.075 µm (samples 826, 827, 829, 830 and 832, is shown in Fig. 13.

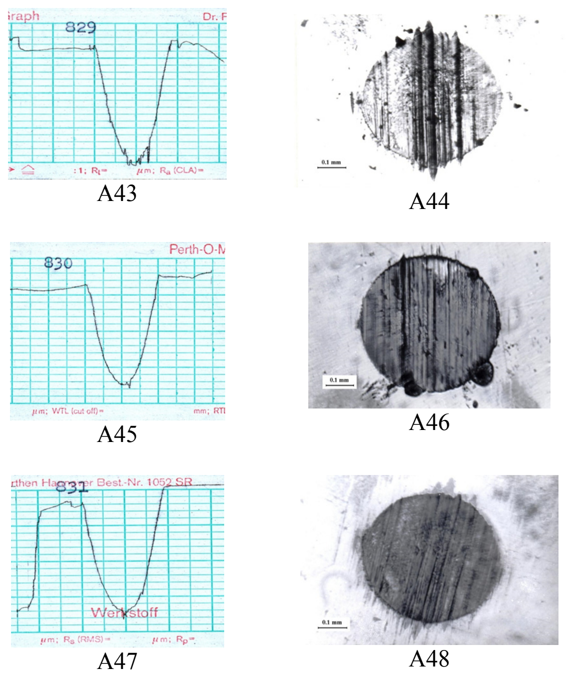

Figure 13. Evolution of the wear function of time, for roughness R_a = 0.075 µm (samples 826, 827, 829, 830 and 832)

Different roughness used have caused not only a diference between worn volume value, but also in the aspect of wear imprint (wear type). In the case of surfaces with R_a = 0.015 µm, R_a = 0.075 µm, (t =3 sec.) and R_a = 0.19 µm, (t =3 sec.), the wear is of adhesive type (metallic shape with prononced scratches). In the case of surfaces with R_a = 0.045 µm, oxidative wear type is prevailling. While reducing the wear rate as a result of surface compliance, surfaces with R_a = 0.075 µm and R_a = 0.19 µm, also goin in oxidative wear regime.

Evolution of the wear function of time, for roughness R_a = 0.19 µm (samples 832, 835, 849, 836, 837 si 850, is shown in Fig. 14.

For roughness R_a = 0.015 µm, R_a = 0.075 µm and R_a = 0.19 µm, the results obtained for the volume of worn material, are consistent with the strain of contact, determined by the lubricant film parameter $h_{\min} / \sigma$.

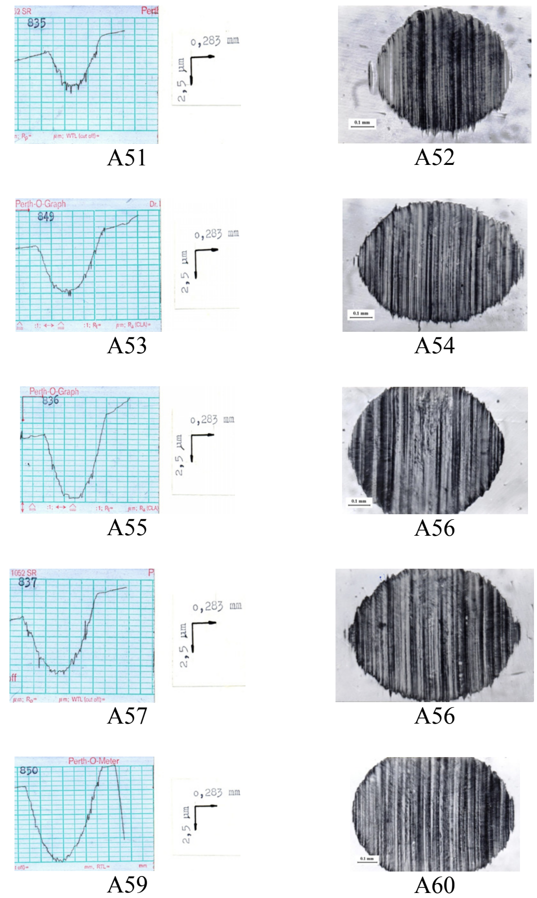

Figure 14. Wear evolutionear function of time, for roughness R_a = 0.19 µm (samples 835, 849, 836, 837 and 850)

For srfaces with roughness R_a = 0.045 µm, there were observed a running-in influence. After the first 5 minutes of operations, the entire contact supraface is covered with oxide. The imprint obtained after another 5 minutes, with the same bush, has a particular form, oxidative wear area restricting the half at outcome ofthe loaded area (samples A52 si A54). It follows that after running, lubrication condition improve.

Figure 15 shows the central profile and the image of wear imprinr (magnification x 68). R_a= 0.15 µm, t =30 min. Pr 997, (new bush).

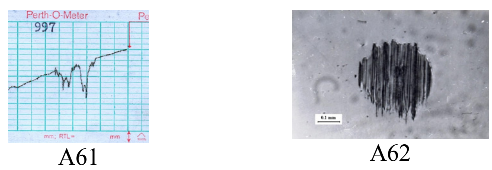

Figure 15. Central transversal profile and image of wear imprint. R_a = 0.15 µm, t = 30 min., sample 997 (new bush).

Next, Figure 16 ilustrates the effect of running on the wear behaviour of the surface with R_a= 0.15

μm, compared with Figure 17, wich shows the effect of running on the wear behaviour of surface with R_a= 0.045 μm.

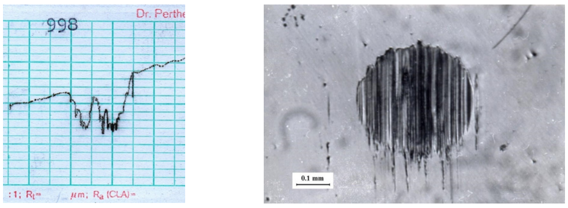

A63 A64

Figure 16. The effect of running-in on the wear behaviour of the surface with R_a= 0.015 μm, t = 5 min, Pr 998. The bush from previous determination was used.

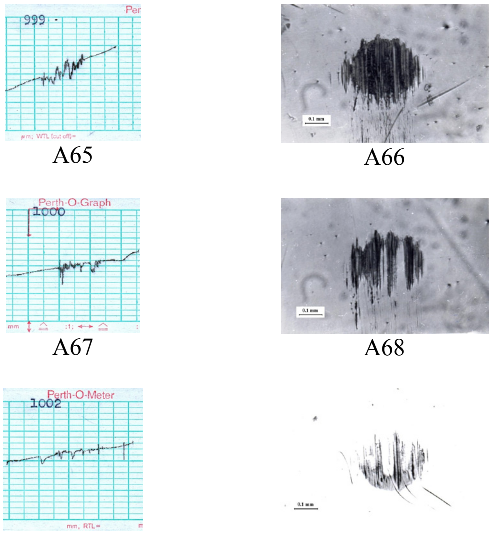

A65 A66

A67 A68

A69 A70

Figure 17. The effect of running-in on the wear behaviour of the surface with R_a= 0.045 μm, t = 5 min, samplez 999, (new bush) 1000 and 1001 (with the bush from previous determination).

Different roughness used has caused not only a difference between worn volume values, but also in the aspect of wear imprint (wear type). In the case of surfaces with R_a = 0.015 μm, R_a = 0.075 μm, (t =3 sec.) and R_a = 0.19 μm, (t =3 sec.), the wear is of adhesive type (metallic shape with pronounced scars). In case of surfaces with R_a = 0.045 μm, oxidative wear type is prevailing. While reducing the wear rate as a result of surface compliance, surfaces with R_a = 0.075 μm and R_a = 0.19 μm also go in oxidative wear regime.

In the case of super-finished surfaces, with R_a = 0.015 μm and R_a = 0.045 μm, a favourable influence of running in is not observed.

For rouhness R_a = 0.015 μm, R_a = 0.075 μm and R_a = 0.19 μm, the results obtained for the volume of worn material, are consistent with the strain of contact, determined by the lubricant film parameter $h_{\min} / \sigma$.

For surfaces with rouhness R_a = 0.045 μm, there was observed a running-in influence. After the first 5 minutes of operation, the entire contact surface is covered with oxide. The imprint obtained after another 5 minutes, with the same bush, has a particular form, oxidative wear area restricting the half at outcome of the loaded area (sample 1001). It follows that after running-in, lubrication conditions improve.

In the case of super-finished surfaces, a favourable influence of running-in is not observed.

4.2. Influence of initial roughness on the wear and friction coefficient

Surface wear, a quantity determined by the fraction of area in contact, should be a monotone function of film parameter h / σ. The minimum value of wear should coincide with the minimum value of surface roughness.

A large number of determinatons of wear, with four roughness have been made: R_a = 0.015 μm; R_a = 0.045 μm; R_a = 0.075 μm si R_a = 0.19 μm. Mean values of volume of worn material for the four roughness are:

R_a = 0.015 μm→V_u = 7.0 x10^{-5} mm^3 → μ = 0.038;
R_a = 0.045 μm→V_u = 7.0 x10^{-6} mm^3 → μ = 0.050;
R_a = 0.075 μm→V_u = 3.7 x10^{-5} mm^3 → μ = 0.038;
R_a = 0.190 μm→V_u = 1.0 x10^{-3} mm^3 → μ = 0.078.

Simultaneously with the surface wear, the friction coefficient was also measured.

In Fig. 18 reprezentative images for three of the four roughnesses are presented.

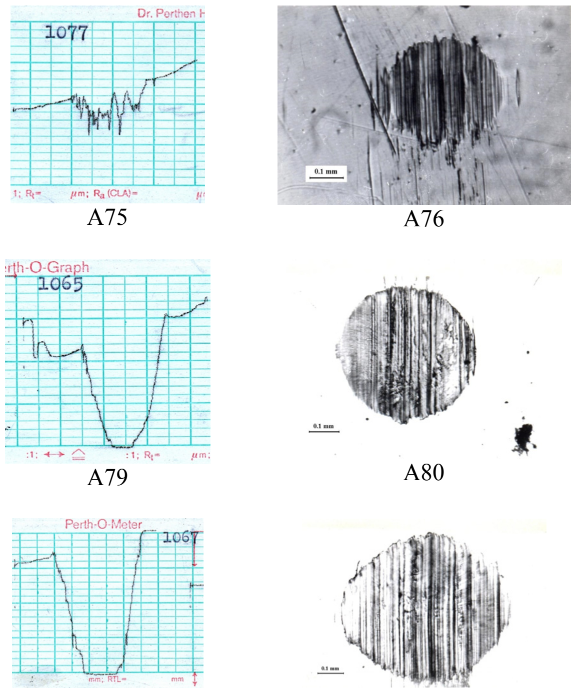

A75 A76

A79 A80

A81 A82

Figure 18. The effect of running-in on the wear behaviour of the surface with R_a= 0.015 μm, t = 5 min, Pr 998. S-a folosit bucsa de la determinarea precedenta.

Existence of an optimal roughness can be explained either by an effect on lubricant film or by a change in mecahanical properties of surface. In this case, at the optimal roughness, reduction of the ratio h / σ is compensed by increase of wear resistence of the surfaces.

5. CONCLUSIONS

From determinatios of the evolution over time of the wear, it resulted that, in the experimental conditions used, minimal wear occurs at a certain valoare of roughness and not at the minimal roughness.

Surprisingly, minimum friction coefficient does not coincide with minimal wear.

The existence of a minimum in the wear curve results for roughness R_a = 0.045 μm. At the same time the friction coefficient is minimal at roughness R_a = 0.045 μm. A mathematical relationship betveen friction coefficient and wear cannot be established.

REFERENCES

[1] B. Katsutoshi, G.E., S. Kiyoshi: US Patent 5092898 / 03.03.1992.

[2] J.P. Davant: *Chirurgie de la hance. Mieux vivre avec une prosthesis.* Fonder l'avenir, 23, pp. 53-56, 1995.

[3] M. Sadeghi-Mehr: *Investigations of Rolling Element Bearing for Hip Joint Prosthesis*, PhD Thesis, Imperial College of Science, Technology and Medicine University. London, 1997.

[4] A. Iarovici, L. Capitanu, V. Florescu, M. Baubec: "*Hip Joint Prosthesis with rolling bodies*", Proceedings of the Romanian Academy – Series A: Mathematics and Physics, Technical Sciences, Information Science, **1**, *1-2*, pp. 37-44, S. 2001.

[5] L. Capitanu, V. Florescu. *New Concepts for Improved Durability in MOM Total Hip Endoprostheses. A review.* American Journal of Materials Science. Vol.2, No. 6, December 2012.

[6] A. Iarovici, L. Capitanu, V. Florescu, M. Baubec, F. Petrescu. *Hip Joint Prosthesis with Rolling Bodies, Part I – The Balls Arrangement Analysis*. Proceedings of the Annual Symposium of the Institute of Solid Mechanics – SISOM, pp. 251-258, 2001,

[7] A. Iarovici, L. Capitanu, V. Florescu, M. Baubec, F. Petrescu. *Hip Joint Prosthesis with Rolling Bodies, Part II – Numerical and Graphical Examples*. Proceedings of the Annual Symposium of the Institute of Solid Mechanics – SISOM, pp. 259-263, 2001.

[8] A. Iarovici, L. Capitanu, J. Onisoru, V. Florescu, M. Baubec. *Stresses and deformations analysis for Hip Joint Prostheses with Rolling Bodies*. Proceeding of the Annual Symposium of the Institute of Solid Mechanics SISOM 2002, pp. 263-268.

[9] Dowson D. *Elastohydrodynamic lubrication. Interdisciplinary Approach to the lubrication of concentrated contacts*. (Ed. P.P.KU) NASA SP – 237, 1970.